Submitted to
Nuclear Physics

LBL-1948
Preprint c.2

DEFORMED STATES OF NEUTRON-DEFICIENT CERIUM AND NEODYMIUM NUCLEI

J. Gizon, A. Gizon, M.R. Maier,
R.M. Diamond and F.S. Stephens

RECEIVED
LAWRENCE
RADIATION LABORATORY

SEP 13 1973

LIBRARY AND
DOCUMENTS SECTION

July 1973

Prepared for the U.S. Atomic Energy Commission
under Contract W-7405-ENG-48

TWO-WEEK LOAN COPY

This is a Library Circulating Copy which may be borrowed for two weeks. For a personal retention copy, call Tech. Info. Division, Ext. 5545

LAWRENCE BERKELEY LABORATORY
UNIVERSITY OF CALIFORNIA
BERKELEY

LBL-1948 c.2

DISCLAIMER

This document was prepared as an account of work sponsored by the United States Government. While this document is believed to contain correct information, neither the United States Government nor any agency thereof, nor the Regents of the University of California, nor any of their employees, makes any warranty, express or implied, or assumes any legal responsibility for the accuracy, completeness, or usefulness of any information, apparatus, product, or process disclosed, or represents that its use would not infringe privately owned rights. Reference herein to any specific commercial product, process, or service by its trade name, trademark, manufacturer, or otherwise, does not necessarily constitute or imply its endorsement, recommendation, or favoring by the United States Government or any agency thereof, or the Regents of the University of California. The views and opinions of authors expressed herein do not necessarily state or reflect those of the United States Government or any agency thereof or the Regents of the University of California.

Nuclear Reactions: $^{120,122}Sn(^{16}O,3n\gamma)$, $^{124}Sn(^{16}O,5n\gamma)$, $^{122,124}Te(^{16}O,3n\gamma)$, E = 60 - 90 MeV; measured $\sigma(E;E_\gamma,\theta)$, γ-γ coincidence, γ-γ delay. $^{133,135}Ce$, $^{135,137}Nd$ deduced levels, J, π, $T_{1/2}$, γ-mixing, prolate shape. Enriched targets, Ge(Li) detectors.

DEFORMED STATES OF NEUTRON-DEFICIENT CERIUM AND NEODYMIUM NUCLEI*

J. Gizon[†‡], A. Gizon[‡], M. R. Maier[‡], R. M. Diamond and F. S. Stephens

Lawrence Berkeley Laboratory
University of California
Berkeley, California 94720

July 1973

Abstract

High-spin levels in Ce and Nd isotopes excited by the reactions $^{120,122}Sn(^{16}O,3n)^{133,135}Ce$ and $^{122,124}Te(^{16}O,3n)^{135,137}Nd$ have been studied by in-beam gamma-ray spectroscopic methods (prompt and delayed spectra, excitation functions, angular distributions and γ-γ coincidences). Bands built on the $11/2^-$ isomeric levels in ^{135}Ce and ^{137}Nd and on the $9/2^-$ ground states in ^{133}Ce and ^{135}Nd have been found. A prolate deformation is required for these nuclei in order to explain the E2/M1 mixing ratios and the level ordering of these bands.

*Work performed under the auspices of the U. S. Atomic Energy Commission.

†NATO fellow.

‡On leave from Institut des Sciences Nucleaires, BP257, Grenoble 38044, France.

‡On leave from Physik Department der TU München, Garching, Germany.

1. Introduction

After the first studies of doubly-even barium isotopes[1]) indicated possible deformed shapes, special attention was directed to the nuclei with N and Z between 50 and 82. The behavior of the high-spin band of levels based on the I = 11/2 state in odd-proton $^{125-133}$La nuclei compared to the energy-spacings of the doubly-even barium isotopes with one less proton[2]) is very striking and has thus far only been interpretable in terms of the particle-plus-rotor model[3]). In order to test further the applicability of this model, experiments on the high-spin states of other nuclei are required. The present paper concerns odd-neutron ^{133,135}Ce and ^{135,137}Nd isotopes studied by observing the γ-radiations following (^{16}O,xn) reactions. In these four nuclei, there is no evidence for a decoupled band having only stretched E2 transitions as was found in the La nuclei. More normal roational bands are seen, though they are still heavily perturbed. It turns out that this is very nearly what is expected for these odd-neutron isotopes according to the above model.

2. Experimental Procedures

The external oxygen beam of the Berkeley 88" sector-focussed cyclotron was used to bombard tin and tellurium targets at 60, 65, 66.5, 70, 80, 85, and 90 MeV energies. The excited levels of ^{135,137}Nd are populated in the ^{122,124}Te(^{16}O,3n) reactions and those of ^{133,135}Ce in the ^{120,122}Sn(^{16}O,3n) reactions, respectively. For ^{135}Ce, we have also used the ^{124}Sn(^{16}O,5n) reaction. The targets were made with enriched isotopes obtained from Oak Ridge National Laboratory and evaporated on 25 μm lead supporting foils. Their thickness was approximately 2 mg/cm^2.

The γ-spectra were recorded using either two 8 cm^3 planar intrinsic germanium detectors with a resolution of 0.9 keV FWHM at 122 keV and 1.9 keV FWHM at 133 keV or with one of the 8 cm^3 planar detectors and a 30 cm^3 coaxial lithium-drifted germanium detector. Their efficiencies were obtained in the actual experimental set up with the γ-rays from calibrated IAEA sources (^{22}Na, ^{57}Co, ^{60}Co, ^{137}Cs) and from ^{177m}Lu samples. The γ-rays were also used for energy calibration, as were the known transitions of the doubly-even nuclei produced in the nuclear reactions. The in-beam γ-rays belonging to ^{135,137}Nd and ^{133,135}Ce are listed in Tables 1-4. The relative gamma intensities given are for an angle of 55° to the incident beam and are normalized to the strongest line, for which $I_\gamma = 100$. For the strong and well-resolved γ-rays, the error is of the order of 0.1% for the energy and about 10% for the intensity. These errors are two or three times higher for the weaker lines.

Singles γ-ray spectra were recorded using the electronic configuration of fig. 1a. Constant fraction triggers[4]) were used to derive timing signals from the detectors. These signals started a time-to-amplitude converter which was stopped by the zero crossing of the cyclotron radiofrequency. A single-channel analyzer was set on the portion taken between the beam pulses (out-of-beam) of the time spectrum and its output signal was used to route corresponding events into different subgroups of the memory of the SCC-660 computer. By this method, the gamma spectra were obtained in-beam and out-of-beam in order to get an indication of isomers and/or decays. During the later experiments the constant fraction triggers were modified[5]) to remove tails on the prompt time curves which allowed better identification of delayed γ-rays.

In the γ-γ coincidence experiments, the arrangement of fig. 1b was used. Events coincident within 300 ns were stored in a 48 events buffer in the PDP-5 computer system. When the buffer was filled, it was written onto magnetic tape. Four parameters were recorded for every coincidence event, the two gamma energies, the time between them and the time between one of the coincident gammas and the zero crossing of the cyclotron RF. The tapes were sorted off line. We set windows on γ-rays in one of the total coincident gamma spectra, on the prompt curve of the γγ-time spectrum and on the in-beam region of the γ-RF time spectrum and accumulated the spectrum from the other detector coincident with the lines selected. Appropriate background windows were also set in the gamma spectra to obtain background spectra which were then subtracted, thus removing coincidences due to the background under the peaks. The accidental coincidences in the γ-γ time spectrum were less than 1% of the true coincidences, so no correction for them was applied. Due to limitations in beam time at the 88" cyclotron, the

later experiments were done using both electronic configurations in parallel; obtaining singles and coincidence spectra simultaneously. The time resolution in the $\gamma\gamma$-time spectrum was usually less than 6 ns FWHM, the resolution in the γ-RF time spectrum was limited by the beam structure to about 10 ns. The single-channel windows for the singles spectra was usually set to give a wide safety margin around the in-beam region, in order to get reliable assignments for the out-of-beam spectra.

The gamma lines were attributed to the final nuclei produced in the $Sn(^{16}O,3n\gamma)Ce$ and $Te(^{16}O,3n\gamma)Nd$ reactions on the basis of excitation functions made with the Ge(Li) detectors at 90° to the beam.

In separate experiments, spectra were recorded at detector angles of 0°, 55° and 90° to the incident beam. From the observed anisotropy we deduced the probable multipolarities of the stronger γ-rays. Since the emitting states may be only partially aligned, the angular distribution function

$$W(\theta) = 1 + \sum_{k \geqslant 2} \alpha_k(I_i)\, A_k^{max}\, (I_i L_1 L_2 I_f)\, P_k(\cos\theta)$$

depends on the attenuation coefficients $\alpha_k(I_i)$. The α_2 coefficients can be deduced by considering the experimental A_2^{exp} coefficients of transitions of known multipolarity, e.g. E2, with the theoretical A_2^{max} for complete alignment tabulated by Yamazaki[6]).

3. Experimental Results

3.1. THE $^{137}_{60}$Nd ISOTOPE

From recent investigations[7-9]) the ground-state of ^{137}Nd has a spin and parity $1/2^+$ and a half-life of (38.5 ± 1.5) m , in agreement with the measurement of Ekström et al.[10]) by the atomic-beam magnetic resonance method. Droste et al.[8]) have identified an isomeric level at 518 keV in ^{137}Nd; gamma-rays of 108, 177, 233 and 285 keV decay with a half-life of (1.60 ± 0.15) s From the γ-ray and conversion-electron intensities, an E3 multipolarity was assigned to the 233 keV isomeric transition. A spin and parity $11/2^-$ for ^{137m}Nd is in agreement with the systematics of N = 77 isotones ^{129}Te, ^{131}Xe, ^{133}Ba, ^{135}Ce, ^{137}Nd and ^{139}Sm, refs. 8 and 11).

The prompt γ-ray spectrum observed in the present study when ^{124}Te is bombarded by 66.5 MeV ^{16}O-particles is shown in fig. 2 and the relative intensities at an angle of 55° to the incident beam are listed in Table 1. In the spectrum taken between beam pulses, the four prominent γ-rays from the isomeric state with energies 108.5, 177.3, 233.4 and 285.8 keV are observed; all the other lines present in this spectrum are associated with the decay of ^{137}Nd to ^{137}Pr, ref. 9).

With an increase in beam energy, the excitation curves of the stronger prompt lines at 328, 407, 581, 669, 706, 794 and 883 keV increase rapidly (fig. 3) indicating high-spin states. From the angular distributions, illustrated in fig. 4, and the A_2^{exp} values reported in Table 1, it is clear that the 581, 706 and 748 keV transitions are mixed dipole-quadrupole radiations where I is lowered by one unit.

It seems obvious that the (669 keV) strongest transition is at the bottom of the prompt cascade. The scheme proposed in fig. 5 has been established from the γ-γ coincidence results, the multipolarities and the intensities of the transitions, and by taking into account the feeding and deexciting of each level.

Within the experimental errors, the intensity balance of the levels below the $11/2^-$ isomeric state is correct. But a small difference appears for the isomeric state when we take the total internal conversion coefficient of the E3 transition into account. This difference can probably be explained by high-energy lines feeding directly into this level. Further up in the band, the $17/2^-$ level is fed principally by a 328.2 keV transition which has a negative A_2^{exp} of -0.20 ± 0.10. This line, which we assume to be a stretched E1 transition (the theoretical value is $A_2^{max} = -0.29$) deexcites a $19/2^+$ state at 2222 keV. We have found a short half-life of 1-4 ns for this level; so the E1 transition of 328 keV is hindered by a factor $(2\text{-}7)\times10^5$ compared to the Weisskopf estimtes. A value of $A_2^{exp} = 0.38 \pm 0.15$ indicates a stretched E2 multipolarity for the 407.2 keV transition which therefore suggests the $23/2^+$, 2630 keV level. The $21/2^-$ and $23/2^-$ levels of the band built on the $11/2^-$ state are weakly fed and we cannot detect higher levels in this band. Because of the strong Pb K_βX-rays and the strong $3/2^+ \rightarrow 1/2^+$, 177.3 keV transition we cannot observe in the singles the $15/2^- \rightarrow 13/2^-$, 87.5 keV and the $19/2^- \rightarrow 17/2^-$, 176.8 keV transitions. In the γ-γ coincidence spectra, the poor statistics also prevent any definite identification. If they do exist, they must be weak.

3.2. THE $^{135}_{58}$Ce ISOTOPE

The ground state of ^{135}Ce has a spin and parity $1/2^+$ [8,12]) and a half-life of 17.0 h. The isomeric level is $11/2^-$ and, as in ^{137}Nd, decays by an E3 transition of 20 seconds half-life[8]). It is now well established that a doublet exists in ^{135}Ce at 296 keV; one of the levels ($3/2^+$) is fed by the decay of ^{135}Pr ($T_{1/2}$ = 27 m)[13-15]) and the other ($5/2^+$) by ^{135m}Ce($T_{1/2}$ = 20 s)[8,13]).

The γ-ray spectra observed during the bombardment of a ^{122}Sn target by 62 MeV ^{16}O-particles are shown in fig. 6. Many γ-rays are present in the spectrum taken between the beam pulses. Besides the 398, 409, 639, 814, 946, and 1125 keV γ-rays, presumably due to an isomer in ^{134}Ce, we can easily identify the lines associated with the decay of ^{135m}Ce and the radioacticity of ^{135}Ce, refs. [16-19]). From the time distributions of the other strongest lines present in the out-of-beam spectrum of 256, 590, 700, 724 and 833 keV, we measured a half-life of 8 ± 2 ns.

The level scheme proposed in fig. 5 has been deduced from the γ-γ coincidences, the intensities, the excitations functions and the multipolarities of the most important lines. A listing of the γ-rays is given in Table 2, but in order to limit its length, we have omitted about 30 lines of low intensity (less than 2% of the strongest). As exceptions, the 109.5 keV (I_γ = 1.2) and the 181.9 keV (I_γ = 0.8) appear in the level scheme: the first is in coincidence with the 590, 724, and 960 keV γ-ray and the second with the 724 keV γ-ray. Definite spins and parities are assigned only to the members of main band built on the $11/2^-$ isomeric level. Taking into account the E3

multipolarity of the 149.6 keV transition, the intensity balance is correct for the isomeric level. Likewise, the balance of the $5/2^+$ level at 296 keV is correct within the experimental errors. So the $3/2^+$ member of the doublet at 296 keV cannot be appreciably excited. This is confirmed by the ratio of the intensities of the 213.4 and 296.1 keV γ-rays which remains constant in the in-beam and out-of-beam single spectra but is quite different from the ratio obtained in the decay of ^{135}Nd, refs. 13,15).

In this nucleus, we find the same kind of excited positive-parity band as in ^{137}Nd. Indeed, from the probable $I = 19/2^+$ level at 2125.6 keV, we reach a $(I = 23/2^+)$ level through the 425.6 keV stretched E2 transition. And, as mentioned before, because of the 8 ns half-life of the former level, all the lower lines in the $11/2^-$ band have such a delayed component. The 256 keV E1 transition is hindered by a factor of 8×10^5 compared to the Weisskopf estimates. We have not seen the 75.0 keV, $19/2^+ \rightarrow 19/2^-$ transition in any spectrum but it should be much weaker than the observed $19/2^+ \rightarrow 17/2^-$ transition.

3.3. THE $^{135}_{60}$Nd ISOTOPE

In previous studies it has been found that the ground state of ^{135}Nd decays to ^{135}Pr with a half-life of 12 to 15 minutes[13,20,21]) while a 5.5 m activity was proposed as an isomeric level in ^{135}Nd. Recently, spin measurements by atomic-beam magnetic resonance[22]) have been performed on samples of praseodymium bombarded with 80 MeV protons and neodymium bombarded with 110 MeV protons. The decays of the $I = 9/2$ resonance signals ascribed to ^{135}Nd were in agreement with a 15 m half-life while nothing has been observed with a 5.5 m half-life.

Spectra recorded when a ^{122}Te target is bombarded with 66.5 MeV ^{16}O-particles are shown in fig. 7. Many lines are detected in the spectrum taken between the beam pulses. The strongest one at 203.8 keV and those at 112, 164, 245, 374, 617 and 661 keV correspond to transitions seen in the decay of ^{135}Nd ($T_{1/2}$ = 15 m). The relative intensities of the γ-rays at 213 and 296 keV are in good agreement with the decay of the $3/2^+$ level at 296 keV in ^{135}Ce, fed from ^{135}Pr ($T_{1/2}$ = 24 m)[13,15]. We have no definite assignment for the other delayed transitions at 109, 414, 423, 476, 502, 539 and 552 keV.

The most intense in-beam line in Table 3 is the 198 keV M1 + E2 transition, and so it must be placed at the bottom of the scheme (fig. 8) where it deexcites the I = 11/2 level to the I = 9/2 ground state. Among the γ-rays in coincidence with this 198 keV line are the 232 and 362 keV M1 + E2 γ-rays. Both are assigned positions in the level scheme based on energy relations and total intensity. The energy and intensity of the 560.5 keV cross-over can be only deduced from the coincidence spectra because of the very strong 564 keV Coulomb excitation line of ^{122}Te. Again, as in the $11/2^-$ bands in ^{137}Nd and ^{135}Ce, the M1 + E2 γ-rays in the I = 9/2 band have very sharp angular distributions. Some other lines, such as the 192 and 518 keV γ-rays, also have negative A_2^{exp} parameters of large magnitude.

3.4. THE $^{133}_{58}$Ce ISOTOPE

Several experiments have been done on the A = 133 neutron-deficient isotopes. In 1967, an isomeric level was identified in ^{133}Ce ref. 23); a (97 ± 4) m half-life was observed for γ-rays at 77, 88, and 97 keV. When

a lanthanum target was bombarded by 95 MeV protons, γ-lines at 173.9, 376.7, 523.4, 556.8, 580.6 and 607.7 keV decayed with the 97 m ^{133m}Ce activity, but all the other γ-rays decayed with a half-life of (5.4 ± 0.05) h.[24]).

The recent in-beam measurements on the odd lanthanum isotopes[2]) established clearly the 11/2$^-$ isomeric level in ^{133}La and the corresponding decay to the ground state of ^{133}La by the 58.2 (E1), 404.6 (M2), 346.4 (M1 + E2), 477.0 (E2) and 130.7 (M1) keV γ-rays. With a lanthanum target irradiated by 95 MeV protons, these five lines are observed and they are associated only with the 5.4 h half-life of ^{133}Ce. On the other hand, in the decay of ^{133}Pr ($T_{1/2}$ = 6.5 m) ⟶ ^{133}Ce ⟶ ^{133}La ref. 25) only the γ-rays of ^{133}La associated with the ^{133m}Ce($T_{1/2}$ = 97 m) decay are found. From the very recent investigations of the spin of the odd-mass isotopes of cerium by atomic-beam magnetic resonance[12]), it appears that I = 9/2 signals correspond to the 5.4 h activity in ^{133}Ce and that I = 1/2 signals can be attributed to the 97 m activity of this isotope. It is not yet known which state is the isomer and which is the ground state.

In the prompt γ-spectrum recorded when a ^{120}Sn target is bombarded with 66.5 MeV ^{16}O-particles (fig. 9) the γ-rays observed in the decay of ^{133}Pr, ref. 25), are missing, except for the 134.3 and 183.4 keV lines. Nevertheless, in the spectrum taken between the beam pulses, the γ-lines following the decay of ^{133}Ce ($T_{1/2}$ = 5.4 h) ⟶ ^{133}La are easily identified. So, taking into account the previous studies, the most intense transitions excited in the ^{120}Sn(^{16}O,3n)^{133}Ce reaction must be placed above the 9/2 level as in the comparable reaction to make ^{135}Nd.

The prompt in-beam γ-spectra of ^{133}Ce and ^{135}Nd are very similar, so it is not surprising that the main parts of the level scheme (fig. 8), established for ^{133}Ce from the experimental results (Table 4), present the same characteristics up to the $23/2^-$ level as for ^{135}Nd. Actually, the similarity of the level spacings in the two nuclei is quite remarkable. To establish the level scheme of ^{133}Ce, we use the same procedure of looking at energy sums, coincidence relations, intensity balance, excitation functions (fig. 10), angular distributions and mixing ratios.

From the 385-609, 609-896, 235-1269 coincidences, the energy sums 554.9 + 608.7 + 896.2 = 2059.8 and 789.7 + 1269.3 = 2059.0, and considering the γ-lines present in the spectrum taken between the beam pulses, we find levels at 1163.6 and 2059.0 keV. The negative value $A_2^{exp} = -0.64 \pm 0.06$ of the 608.7 keV γ-ray which terminates at the I = 13/2 level suggests a spin I = 15/2 level for the 1163.6 keV level. The 896 keV line, which has a stretched E2 character, then gives rise to an I = 19/2 level having the same parity as that at 1163 keV. Above the 2059 keV level, we indicate a set of levels obtained on the basis of γ-γ coincidences and intensity rules. Four of these γ-rays have negative A_2^{exp} coefficients indicating transitions of mixed dipole-quadrupole character. This side band decays into the $9/2^-$ band with a very short half-life ($T_{1/2} \lesssim 3$ ns).

4. Mixing Ratios

In Tables 1-4, the values of the A_2^{exp} coefficients, neglecting A_4, are indicated when the gamma lines are well resolved and the statistics good enough. The delayed γ-rays below the $11/2^-$ isomeric state in ^{137}Nd and ^{135}Ce for which $\alpha_k = 0$ give a determination of the experimental isotropic angular distribution. The attenuation coefficients α_2 are deduced from experimental results on the pure E2 transitions between levels of the bands built on the $11/2^-$ level in ^{137}Nd and ^{135}Ce and on the $9/2^-$ level in ^{135}Nd and ^{133}Ce. Since we did not find trends in α_2 with spin, we averaged the α_2 values for each nucleus in order to reduce their scatter. For ^{135}Nd and ^{137}Nd, the mean values of α_2 are 0.43 ± 0.16 and 0.44 ± 0.20, respectively. In the cases of the two cerium nuclei, the attenuation coefficients are much larger and reach 0.69 ± 0.19 for ^{133}Ce and 0.76 ± 0.19 for ^{135}Ce.

Using the mean α_2 coefficient for each nucleus, it is possible to determine the quadrupole to dipole amplitude mixing ratio δ of M1 + E2 transitions. Some values of experimental A_2^{max} are obtained with a large error, but all the results are consistent with a large negative value around one. This results from the fact that all the M1 + E2 transitions in the $11/2^-$ and $9/2^-$ bands are characterized by a very "sharp" angular distribution. Examples of such very sharp angular distributions are given in fig. 4, where we can see the great difference in the intensities of the peaks at 0° and 90° relative to the beam. In fig. 11, two theoretical A_2^{max} values are represented as functions of $|\delta|/(1 + |\delta|)$. Roughly, we can say that the multipolarity of these M1 + E2 transitions is an admixture with (50 ± 25)% E2. The mixing ratios δ equals -1.0 when A_2^{max} reaches its extremum, $A_2^{max} \simeq -1.2$.

Thus, in all the cases with such large negative A_2^{exp}, the sign of δ is negative. Using the results[26]) on ^{199}Tl, Nakai[27]) pointed out the fact that

$$\text{sign } \delta = \text{sign } \left(\frac{g-g_R}{Q_0}\right) \qquad \text{for } K \neq 1/2 \quad ,$$

$g-g_R$ is positive for odd-proton nuclei and negative for odd-neutron nuclei provided $I \geqslant 7/2$.

In the cases discussed here, δ is negative for all M1 + E2 transitions in the $9/2^-$ and $11/2^-$ bands of these odd-neutron nuclei. Consequently, Q_0 must be positive indicating that, the nuclei are all prolate.

5. Discussion

As shown in figs. 5 and 8, the level structure of Ce and Nd nuclei are quite similar for a given neutron number. So we shall consider the four nuclei in pairs: ^{135}Ce and ^{137}Nd with 77 neutrons and ^{133}Ce and ^{135}Nd with 75 neutrons.

5.1. FEEDING OF THE LEVELS

From the experimental results, we deduce the following:

i) The levels of the $1/2^+$ ground-state band in both ^{135}Ce and ^{137}Nd are only populted with appreciable intensity by deexcitation of the $11/2^-$ isomeric state. We do not observe any γ-rays in coincidence with the 213 and 296 keV in ^{135}Ce or with the corresponding 109 and 286 keV in ^{137}Nd. In addition, the sum of the intensities of the E2 ($5/2^+ \rightarrow 1/2^+$) and of the M1 + E2 ($5/2^+ \rightarrow 3/2^+$) transitions equals the total intensity of the E3 ($11/2^- \rightarrow 5/2^+$) transition.

ii) The levels of these $11/2^-$ bands are fed by the decay of higher states in the band only up to about spin $19/2^-$. The side-band with spins $19/2^+$ and $23/2^+$ comes below the expected position of the $21/2^-$ level so it seems reasonable that the levels with $I \geqslant 21/2$ in the $11/2^-$ bands are populated only weakly.

iii) In the four nuclei, we observe that the intensity of the stretched E2 ($I + 2 \rightarrow I$) cross-over and of the M1 + E2 ($I + 1 \rightarrow I$) transition is stronger when I+1/2 is even; this is a result of the level spacing and the strong energy dependence of the transition probabilities. These energy spacings are due to the $h_{11/2}$ origin of the negative-parity states.

iiii) The $17/2^-$ levels in ^{135}Ce and ^{137}Nd are fed from states at 2126 and 2122 keV, respectively i.e. in the same energy range as a 5^- state in the doubly-even $^{136,138}Ce$ and $^{138,140}Nd$. The half-life of this level is (8 ± 2) ns in ^{135}Ce and smaller than 4 ns for ^{137}Nd. The analogous states are probably too high to be easily observed in ^{133}Ce and ^{135}Nd. The structure of these 5^- states is unknown. In some neutron-deficient nuclei of Sn and Te, there is also a 5^- state whose energy and half-life increase as the mass number decreases. These states might be related to the ones in the Ce-Nd region. The only known odd-A nucleus in this region which presents an analogy is ^{131}Ce, ref. [28]), which has precisely the same neutron number. It also has a $19/2^+$ level decaying by hindered E1 transitions to negative parity states.

5.2. PROLATE SHAPE

It was shown[29]) that the level structure of some moderately deformed odd-A gold nuclei could be explained by a particle-plus-rotor model. Since the Fermi surface in that case,,(as in the present Ce-Nd case), was above the $h_{11/2}$ sub-shell, observation experimentally of "decoupled" bands having the energy spacings of the ground band in the neighboring doubly-even nuclei required oblate shapes. On the other hand, prolate shapes require bands with the normal ($\Delta I = 1$) spin sequence and energy spacings that favor the $I = j$ $j + 2$, $j + 4$, $\cdots$ spin states at low deformation, but become the usual $I(I + 1)$ rotational values at large deformations.

The negative-parity bands found in Ce and Nd are clearly not like the decoupled bands in the odd-proton gold nuclei, but are like the perturbed rotational bands expected for prolate shapes. Indeed the ratio of the

transition energy ($E_{15/2} - E_{11/2}$) to that of the mean value of the $2^+ \rightarrow 0^+$ transitions of the neighboring doubly-even nuclei is of the order of 1.5 rather than 1 as is found for the decoupled bands and the level spacings become more rotational as the mass number decreases (deformation increases)

The quantitative agreement between experiment and calculation in these Ce, Nd nuclei is not as good as in the earlier cases, but the reason is probably due to the occurrence of asymmetric shape effects such as γ-distortion or softness. Such γ-distortion effects are indicated by the low-lying second 2^+ state in the doubly-even nuclei in this region. This 2^+ state is so low that it falls below the 4^+ of the ground-state band. Such γ-softness could produce deviations in the level spacings from those of the axially-symmetric particle-plus-rotor model used in the calculation, and it can be shown that such deviations are in the direction of the experimental data.

In summary, it appears that the properties of the $11/2^-$ and $9/2^-$ bands observed in these Ce and Nd nuclei are qualitatively in good agreement with what would be expected from the particle-plus-rotor model calculated for prolate shapes. The difference between the odd-A La nuclei, which show decoupled spectra, and the present odd-mass nuclei, which show more normal rotational bands, is that the Fermi surface lies below the $h_{11/2}$ orbital for the odd-proton nuclei in this region rather than above it as for the odd-neutron nuclei. It appears that this simple model can give considerable insight into the high-spin states of nuclei in this region of intermediate deformation.

Acknowledgments

We would like to thank Drs. E. Grosse and D. Proetel for their help in many phases of this study. We are indebted to the 88" Cyclotron crew for providing the ^{16}O beams. Three of us (J.G., A.G., and M.R.M.) appreciated the opportunity to participate in this experiment at the Lawrence Berkeley Laboratory. J. Gizon wants to thank NATO for supplying the fellowship for his stay.

References

1) R. K. Sheline, T. Sikkeland and R. N. Chanda, Phys. Rev. Letters 7 (1961) 446

2) J. R. Leigh, K. Nakai, K. H. Maier, F. Pühlhofer, R. M. Diamond and F. S. Stephens, to be published in Nucl. Phys.

3) F. S. Stepehns, R. M. Diamond, J. R. Leigh, T. Kammuri and K. Nakai, Phys. Rev. Letters 29 (1972) 438

4) M. R. Maier and P. Sperr, Nucl. Instr. Methods 87 (1970) 13

5) M. R. Maier and D. A. Landis, to be published in Nucl. Instr. Methods

6) T. Yamazaki, Nucl. Data A3 (1967) 1

7) Z. Zhelev, V. G. Kalinnikov and N. A. Lebedev, Contrib. Intern. Conf. Nucl. Struct. Dubna, D. 3393 (1968) p. 22

8) Ch. Droste, W. Neubert, J. Lewitowicz, S. Chojnacki, T. Morek, Z. Wilhelmi, and K. F. Alexander, Nucl. Phys. A152 (1970) 579

9) V. S. Butsev, Ts. Vylov, K. Ya. Gromov, V. G. Kalinnikov, I. I. Gromova, V. A. Morozov, T. M. Muminov, H. Fuia and A. B. Khalikulov, J.I.N.R. P6 6804, Dubna (1972)

10) C. Ekström, S. Ingelman, M. Olsmats, B. Wannberg, G. Andersson and A. Rosen, Nucl. Phys. A196 (1972) 178

11) J. Van Klinken, S. Goring, D. Habs, M. von Hartrott, H. Klewe-Nebenius, R. Löhken, H. Rebel and G. Schatz, Z. Physik 246 (1971) 369

12) S. Engelmann, C. Ekström, M. Olsmats and B. Wannberg, to be published in Physica

13) A. R. Brosi and B. H. Ketelle, ORNL - 4306 (1968) p. 7

14) A. A. Abdurazakov, A. Arlt, R. Babadzmanov, G. Baier, V. A. Morozov, G. Musiol, Kh. Tyrroff and H. Strusny, Izv. Akad. Nauk. SSSR. 34 (1970) 796; 34 (1971) 706.

15) R. Arlt, G. Beyer, V. A. Morozov, G. Musiol, T. M. Muminov, H. Tyrroff, H. Strusny, Z. A. Usmanova, V. I. Fominyki, H. Fuia, A. B. Khalibulov and E. Herrmann, J.I.N.R. P6-6217, Dubna (1972) and Intern. Conf. Nucl. Struct. Kiev (1972) p. 99

16) A. Abdul-Malek and R. A. Naumann, Phys. Rev. 166 (1968) 1194

17) Z. G. Gritchenko, T. P. Makarova, Yu. Ts. Oganesyan, Yu. E. Penionzhkevitch and A. V. Stepanov, Sov. J. Nucl. Phys. 10 (1970) 536

18) V. Zhuk, E. Krupa, V. A. Morozov, T. M. Muminov, H. Fuia,and A. B. Khalikulov, J.I.N.R. P6-6040, Dubna (1971)

19) F. Bazan and R. A. Meyer, Nucl. Phys. A164 (1971) 552

20) R. Arlt, V. A. Bystov, W. Habenicht, E. Herrmann, V. I. Raiko, H. Strusny and H. Tyrroff, Nucl. Instr. Methods 102 (1972) 253

21) R. Arlt, G. Baier, H. Tyrroff, Z. A. Usmanova, H. Strusny and E. Herrmann, Contrib. Intern. Conf. Nucl. Structure, Kiev (1972) 100

22) C. Ekström, S. Ingelman, M. Olsmats and B. Wannberg, Nucl. Phys. A196 (1972) 178 and C. Ekström private communication, Feb. 1973

23) C. Gerschel and G. Albouy, C. R. Acad. Sci. B264 (1967) 183

24) C. Gerschel, Nucl. Phys. A108 (1968) 337

25) R. Arlt, G. Beyer, K.Ya. Gromov, G. Musiol, H. G. Ortleff, H. Tyrroff, Z. A. Usmanova, H. Strusny and E. Herrmann, J.I.N.R. P6-6285, Dubna 1972

26) J. O. Newton, S. D. Cirilov, F. S. Stephens and R. M. Diamond, Nucl. Phys. A148 (1970) 593

27) K. Nakai, Phys. Letters 34B (1971) 269

28) A. Kerek, A. Luukko, M. Grecescu and J. Sztarkier, Nucl. Phys. A172 (1971) 603

29) F. S. Stephens, R. M. Diamond, D. Benson, Jr. and M. R. Maier, Phys. Rev. C7 (1973) 2163

Table I. Gamma-Rays of ^{137}Nd Produced in the $^{124}Te(^{16}O,3n\gamma)^{137}Nd$ Reaction at 66.5 MeV.

E_γ (keV)	Relative Gamma Intensity	A_2^{exp}	Multipolarity	Transition Assignment
108.7	56.0	-0.03 ± 0.10	M1 + E2[a)]	$5/2^+ \rightarrow 3/2^+$
138.1	4.4			
159.5	5.3			
177.3	100.0	-0.01 ± 0.10	M1 + E2[a)]	$3/2^+ \rightarrow 1/2^+$
				$(19/2^- \rightarrow 17/2^-)$
195.6	3.3			
209.0	3.0			
213.1	5.2			
233.4	93.5	-0.01 ± 0.10	E3 [a)]	$11/2^- \rightarrow 5/2^+$
263.9	5.4			
268.3	4.5			
285.9	35.6	+0.05 ± 0.11	E2 [a)]	$5/2^+ \rightarrow 1/2^+$
294.4	4.4			
308.3	10.6			
328.2	27.7	-0.20 ± 0.10	E1	$19/2^+ \rightarrow 17/2^-$
332.1	6.7			
353.9	5.4			
389.1	9.1			
407.2	19.1	+0.38 ± 0.15	E2	$23/2^+ \rightarrow 19/2^+$
409.7	6.3			
414.2	2.1			
418.2	11.6			
440.1	30.2			
449.1	2.4			
453.9	1.8			
460.2	5.2			
517.3	2.4			

(continued)

Table I. (cont.)

E_γ (keV)	Relative Gamma Intensity	A_2^{exp}	Multipolarity	Transition Assignment
520.5	5.8			
525.0	5.0			
548.4	3.7			
552.2	6.9			
556.7	3.2			
563.4[b)]	4.8			
574.9	4.3			
581.4[c)]	41.2	-0.69 ± 0.05	M1 + E2	$13/2^- \rightarrow 11/2^-$
668.9	51.6	+0.19 ± 0.12	E2	$15/2^- \rightarrow 11/2^-$
682.0	2.9			
705.9	30.2	-0.85 ± 0.03	M1 + E2	$17/2^- \rightarrow 15/2^-$
729.1	8.6			
748.4	7.3	-0.53 ± 0.09	M1 + E2	$21/2^- \rightarrow 19/2^-$
759.0	7.2			
770.7	7.3			
779.2	3.0			
793.7	15.1	+0.14 ± 0.14	E2	$17/2^- \rightarrow 13/2^-$
882.9	21.4	+0.23 ± 0.18	E2	$19/2^- \rightarrow 15/2^-$
924.5	7.4		(E2)	$21/2^- \rightarrow 17/2^-$
1009.3	8.2		(E2)	$23/2^- \rightarrow 19/2^-$
1012.5	6.2			

a) The multipolarities of the transitions below the $11/2^-$ isomeric level were previously known.

b) Composite line.

c) A small component of this line belongs to ^{137}Pr.

Table II. Gamma-Rays of ^{135}Ce Produced in the $^{122}Sn(^{16}O,3n\gamma)^{135}Ce$ Reaction at 62 MeV.

E_γ (keV)	Relative Gamma Intensity[a)]	A_2^{exp}	Multipolarity	Transition Assignment
103.3	3.0			
125.0	2.5			
149.7	24.9	-0.02 ± 0.06	E3[b)]	$11/2^- \rightarrow 5/2^+$
159.6	54.1			
169.6	8.4			
175.0	4.8	-0.44 ± 0.09	M1 + E2	3129.7 → 2954.7
189.4	8.9			
202.1	11.1	-0.38 ± 0.08	M1 + E2	2686.8 → 2484.7
206.9	6.4			
213.4	100.0	+0.04 ± 0.01	M1 + E2[b)]	$5/2^+ \rightarrow 3/2^+$
238.1	2.0			
248.9	2.1			
256.0	30.2	-0.26 ± 0.08	(E1)	$(19/2^+ \rightarrow 17/2^-)$
262.2	3.7			
267.9	4.8	-0.46 ± 0.09	M1 + E2	2954.7 → 2686.8
277.0	3.5			
285.0	2.0			
296.1	25.0	-0.04 ± 0.08	E2[b)]	$5/2^+ \rightarrow 1/2^+$
309.0[b)]	5.3			
325.4	4.6			
334.8	3.0			
358.3	3.4	-0.42 ± 0.11	M1 + E2	$2484.7 \rightarrow 19/2^+$
376.0	3.3			
379.4	10.4			2484.7 → 2105.3
381.6	5.8			
384.5	8.4			
391.8	7.0			

(continued)

Table II. (cont.)

E_γ (keV)	Relative Gamma Intensity[a)]	A_2^{exp}	Multipolarity	Transition Assignment
404.0	5.4			
417.2	7.9			
423.0	4.8			
425.6	25.6	+0.28 ± 0.16	E2	$(23/2^+ \rightarrow 19/2^+)$
428.5	4.4			
433.4	7.7	-0.63 ± 0.06	M1 + E2	2105.3 → 1670.6
440.0	4.4			
446.8	3.5			
451.9	6.8			
464.7	11.7			
498.6	4.0			
511.0	46.5			
521.5	4.3			
533.3	7.4			
557.0	14.4			
569.7[c)]	15.5			
577.9	5.4			
580.1	14.9			
584.4	3.0			
589.7	47.2	-0.71 ± 0.04	M1 + E2	$13/2^- \rightarrow 11/2^-$
595.5	6.8			
603.8	26.1			
616.0	6.1			
620.8	4.3			
628.0	6.3			
635.2	17.6	-0.30 ± 0.10	(M1 + E2)	$1670.6 \rightarrow 13/2^-$
647.0	12.2			
665.2[b)]	5.0			

(continued)

Table II. (cont.)

E_γ (keV)	Relative Gamma Intensity[a)]	A_2^{exp}	Multipolarity	Transition Assignment
668.3	10.9			
678.9	15.1			
699.6	73.5	+0.35 ± 0.11	E2	$15/2^- \rightarrow 11/2^-$
724.3	36.6	-0.79 ± 0.03	M1 + E2	$17/2^- \rightarrow 15/2^-$
734.9	2.6			
741.5	4.5			
745.2	6.6			
753.9[c)]	4.8			
770.1	6.7			
783.3	8.0			
786.9	6.0			
827.7	3.4			
833.1	16.3	+0.31 ± 0.13	E2	$17/2^- \rightarrow 13/2^-$
862.7	3.9			
875.4	3.5			
885.4	5.7			
888.2	5.1			
894.7	4.2			
897.6	3.2			
906.2[c)]	21.0	+0.30 ± 0.18	E2	$19/2^- \rightarrow 15/2^-$
927.3	8.9			
940.3	2.6			
960.0	4.2			
964.1[c)]	21.0			
977.7	6.3			
1000.5	9.2			
1004.9	3.3			
1012.7[c)]	4.7			

(continued)

Table II. (cont.)

E_γ (keV)	Relative Gamma Intensity [a]	A_2^{exp}	Multipolarity	Transition Assignment
1019.0	5.3			
1029.3[b]	7.1			
1052.0	9.5			
1197.4	5.5			
1368.7	25.0			

[a] Gamma-rays with a relative intensity smaller than 2 are not listed.

[b] The multipolarities of the transitions below the isomeric state were previously known.

[c] Composite line.

Table III. Gamma-Rays of ^{135}Nd Produced in the $^{122}Te(^{16}O,3n\gamma)^{135}Nd$ Reaction at 66.5 MeV.

E_γ (keV)	Relative Gamma Intensity[a)]	A_2^{exp}	Multipolarity	Transition Assignment
108.7	4.3			
120.4	2.0			
128.2	7.1			
137.9	4.3			
158.7	4.3			
169.8	9.6			
176.7	7.0			
178.2				
192.0	13.2			
198.5	100.0	-0.64 ± 0.03	M1 + E2	$11/2^- \rightarrow 9/2^-$
207.4	18.4			
232.2	12.7	-0.68 ± 0.04	M1 + E2	$15/2^- \rightarrow 13/2^-$
234.9	2.9			
243.1	5.1			
247.7	6.7			
250.6	1.8		(M1 + E2)	$19/2^- \rightarrow 17/2^-$
256.2	2.9			
282.0	6.4			
284.9	2.9			
290.9	3.0			
300.9	4.4	-0.27 ± 0.15	M1 + E2	$23/2^- \rightarrow 21/2^-$
325.3	9.5			
362.2	39.5	-0.65 ± 0.05	M1 + E2	$13/2^- \rightarrow 11/2^-$
410.3	7.8			
422.8	3.1			
440.4	38.3			

(continued)

Table III. (cont.)

E_γ (keV)	Relative Gamma Intensity [a]	A_2^{exp}	Multipolarity	Transition Assignment
476.0	22.6			
476.5		-0.42 ± 0.09	M1 + E2	$17/2^- \rightarrow 15/2^-$
482.6	6.8			
501.8	9.6			
511.8	117.0			
518.3	12.0			
525.7	4.3			
533.5	7.4			
552.1	9.8			
554.1	6.4			
560.3	18 [b]		(E2)	$13/2^- \rightarrow 9/2^-$
585.0	8.8	-0.53 ± 0.08	M1 + E2	$21/2^- \rightarrow 19/2^-$
594.1	33.4	+0.14 ± 0.11	E2	$15/2^- \rightarrow 11/2^-$
646.9	4.0			
670.7	2.8			
709.6	12.1	+0.11 ± 0.14	E2	$17/2^- \rightarrow 13/2^-$
727.6	19.6	+0.18 ± 0.13	(E2)	$19/2^- \rightarrow 15/2^-$
747.8	4.2			
752.6	2.8			
814.8	4.6			
835.7	7.6	+0.28 ± 0.15	E2	$21/2^- \rightarrow 17/2^-$
855.7	6.9			
886.0	14.5		(E2)	$23/2^- \rightarrow 19/2^-$
888.4				
1015.5	10.0			
1060	5.7			
1161	11.2			

[a] Gamma-rays with a relative intensity smaller than 2 are not listed.
[b] Intensity deduced from the γ-γ coincidence spectra.

Table IV. Gamma-Rays of ^{133}Ce Produced in the $^{120}Sn(^{16}O,3n\gamma)^{133}Ce$ Reaction at 65 MeV.

E_γ (keV)	Relative Gamma Intensity [a]	A_2^{exp}	Multipolarity	Transition Assignment
134.3	7.2			
154.7	3.4			
159.5	23.6	-0.35 ± 0.06	M1 + E2	2218.5 → 2059.0
170.0	100.0	-0.55 ± 0.04	M1 + E2	$11/2^- \rightarrow 9/2^-$
183.6	4.8			
189.5	20.9	-0.39 ± 0.06	M1 + E2	2408.0 → 2218.5
197.3	4.4			
200.7	19.1	-0.38 ± 0.07	M1 + E2	2608.7 → 2408.0
205.4	4.6			
208.9	1.3			
215.4	2.2			
223.8	7.1			
234.8	31.9	-0.46 ± 0.07	M1 + E2	$15/2^- \rightarrow 13/2^-$
240.8	9.0			
246.0	3.6		(M1 + E2)	$19/2^- \rightarrow 17/2^-$
252.6	2.2			
276.8	2.6			
283.1	6.9			
294.9	17.9	-0.42 ± 0.06	M1 + E2	2903.6 → 2608.7
302.9	7.3			
357.5	13.7	-0.07 ± 0.11		3261.1 → 2903.6
384.7	63.8	-0.61 ± 0.05	M1 + E2	$13/2^- \rightarrow 11/2^-$
390.6	5.5			
400.0	5.3			
416.2	2.8			
423.0	6.9			
435.9	4.6			
444.4	8.2			

(continued)

Table IV. (cont.)

E_γ (keV)	Relative Gamma Intensity [a]	A_2^{exp}	Multipolarity	Transition Assignment
457.6	5.0			
464.6	5.2			
496.8	9.5			
507.7	7.3			
511.0	18.6			
516.7	21.1	-0.75 ± 0.04	M1 + E2	$17/2^- \rightarrow 15/2^-$
530.2	5.0			
544.2	7.9			
553.1	4.4			
554.9	12.9	+0.19 ± 0.14	E2	$13/2^- \rightarrow 9/2^-$
562.3	5.8			
563.7	15.5			
570.1	9.3			
577.3	7.5			
582.2	4.7			
608.7	14.5	-0.64 ± 0.06	M1 + E2	$1163.6 \rightarrow 13/2^-$
617.3	15.0			
619.7	65.6	+0.30 ± 0.15	E2	$15/2^- \rightarrow 13/2^-$
624.8	3.4			
630.1	4.6			
644.4	4.4		(M1 + E2)	$(21/2^- \rightarrow 19/2^-)$
691.9	7.3			
706.3	3.9			
751.3[b)]	21.4	+0.33 ± 0.15	E2	$17/2^- \rightarrow 13/2^-$
762.6	28.4	+0.34 ± 0.14	E2	$19/2^- \rightarrow 15/2^-$
794.7	10.8			
798.0	4.0			
817.3	3.4			

(continued)

Table IV. (cont.)

E_γ (keV)	Relative Gamma Intensity [a]	A_2^{exp}	Multipolarity	Transition Assignment
855.7	9.3			
891.0	4.0		(E2)	$(21/2^- \rightarrow 17/2^-)$
896.2	16.6	+0.15 ± 0.14		2059.0 → 1163.6
908.0	5.5			
913.5	4.4			
954.0	16.4	+0.00 ± 0.20		$(23/2^- \rightarrow 19/2^-)$
957.0	5.2			
981.6	6.6			
1023.4	8.0			
1071.9	8.8			
1075.8	5.6			
1190.7	11.3			
1269.3	29.9			$2059.0 \rightarrow 15/2^-$
1304.5	8.3			

[a] Gamma-rays with a relative intensity smaller than 2 are not listed.

[b] This line could be composite.

Figure Captions

Fig. 1. Block diagram of the electronic arrangement. The set-ups a and b are used for single γ-rays and γ-γ coincidence spectra, respectively. D1,D2 = detectors. PA = preamplifier, cooled FET. HV = High voltage supply. MA = main amplifier. FPO = fast pick off amplifier. PUR = pile up rejector. LG = linear gate. CF = constant fraction trigger. TAC = time to amplitude converter. FI = fan in (or gate). RFP = radio frequency zero pick off. ADD = Adding amplifier. SCA = scaler. ADC = analog digital converter. MPX = multiplexer.

Fig. 2. In-beam and out-of-beam γ-ray spectra observed at 90° to the beam in the $^{124}Te + ^{16}O$ reaction at 66.5 MeV. The asterisks indicate γ-rays in ^{137}Pr.

Fig. 3. Relative excitation functions of ^{137}Nd γ-rays.

Fig. 4. Example showing the sharp angular distribution of the 581.4 and 705.9 keV γ-rays in ^{137}Nd. The lower spectrum has been shifted down by a factor of 60.

Fig. 5. Level schemes of ^{137}Nd and ^{135}Ce. The widths of the arrows are proportional to the total intensities of the transitions. The transitions within the $11/2^-$ band are solid.

Fig. 6. In-beam and out-of-beam γ-ray spectra observed at 90° to the beam in the $^{122}Sn + ^{16}O$ reaction at 62 MeV.

Fig. 7. In-beam and out-of-beam γ-ray spectra observed at 90° to the beam in the $^{122}Te + ^{16}O$ reaction at 66.5 MeV. The asterisks indicate that the lines belong to ^{135}Pr.

Fig. 8. Level schemes of ^{135}Nd and ^{133}Ce. The widths of the arrows are proportional to the total intensities of the transitions. The transitions within the $9/2^-$ bands are solid.

Fig. 9. In-beam and out-of-beam γ-ray spectra observed at 90° to the beam in the $^{120}Sn + ^{16}O$ reaction at 66.5 MeV.

Fig. 10. Relative excitation functions of ^{133}Ce γ-rays.

Fig. 11. Examples of determination of quadrupole to dipole amplitude mixing ratio, δ, of M1 + E2 transitions in ^{133}Ce from the experimental A_2^{max} angular distribution coefficients. The solid curves represent the theoretical A_2 coefficients versus $|\delta|/(1+|\delta|)$ for complete alignment; the hatched area represent the experimental value of A_2 corrected for attenuation of the 170.0 keV, $11/2^- \rightarrow 9/2^-$ and 384.7 keV, $13/2^- \rightarrow 11/2^-$ transitions.

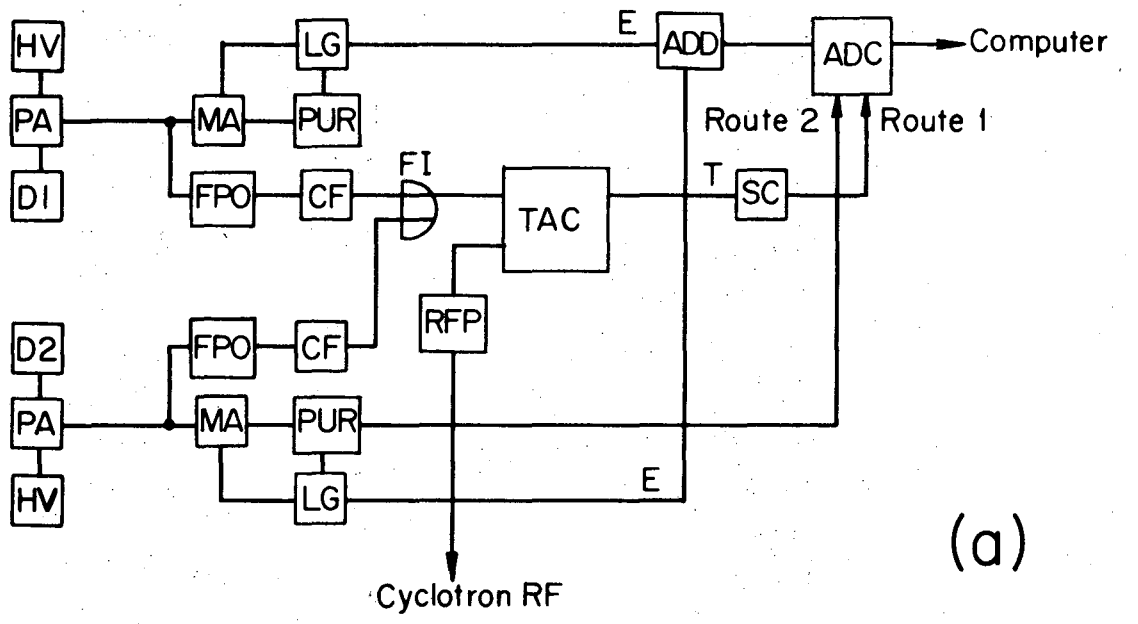

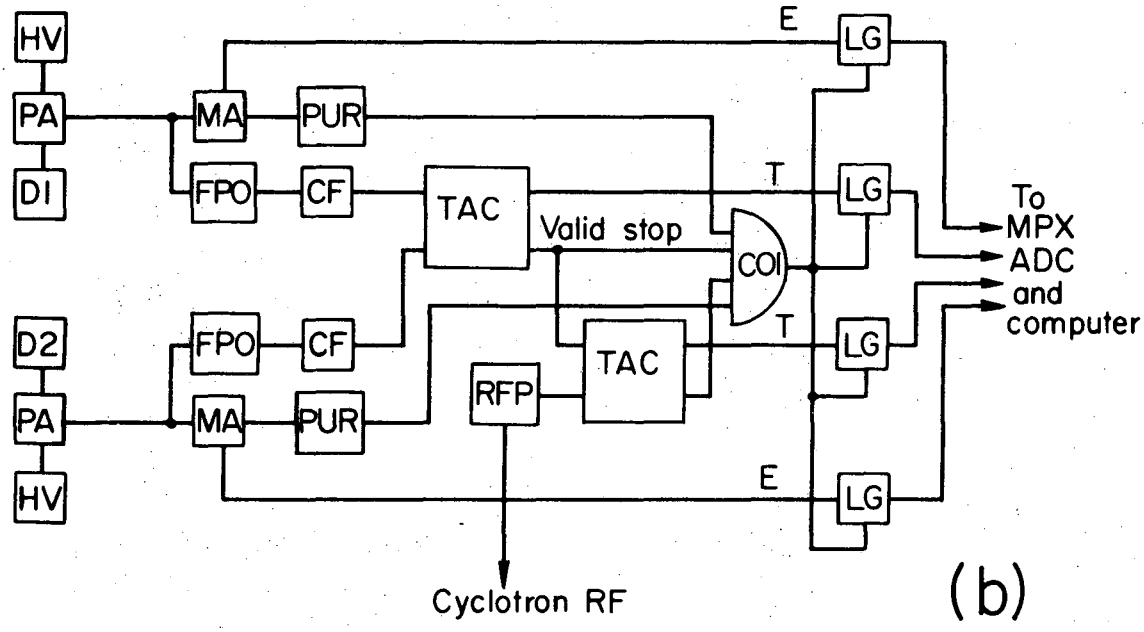

XBL 737-3318

Fig. 1

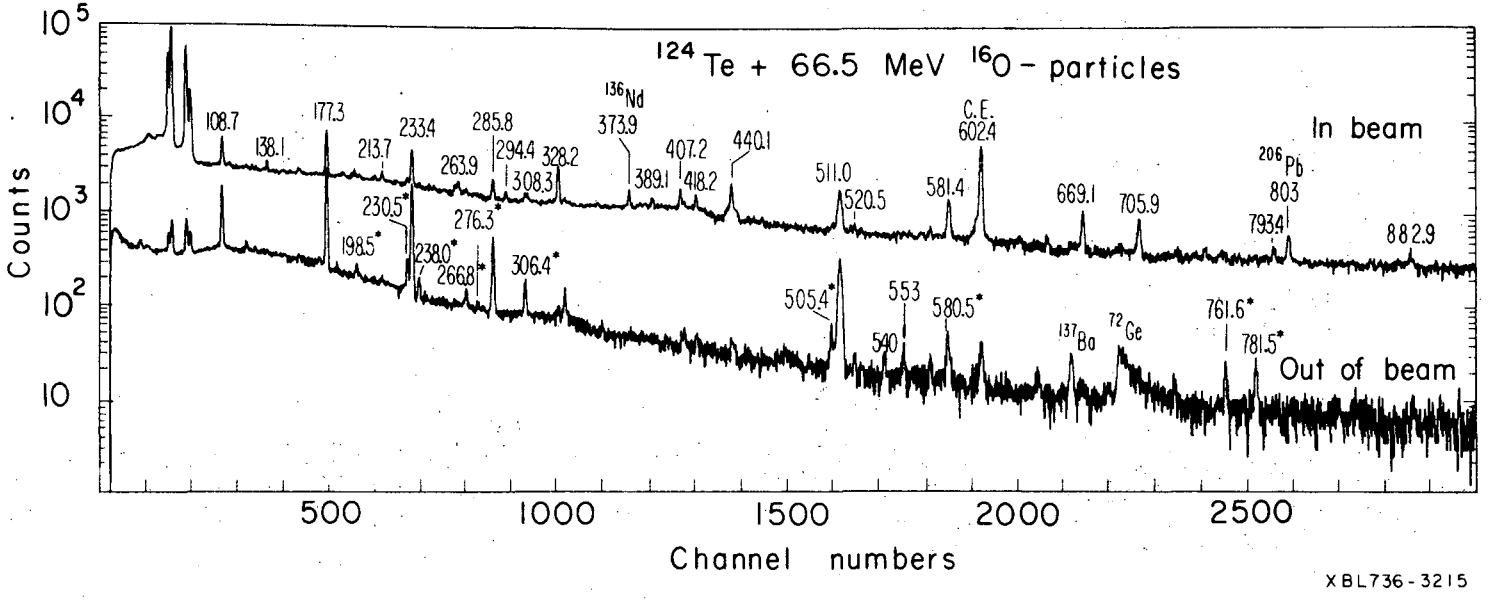
124 Te + 66.5 MeV 16O - particles
In beam
Out of beam
Counts
Channel numbers
10
10^2
10^3
10^4
10^5
500
1000
1500
2000
2500
108.7
138.1
177.3
213.7
233.4
263.9
285.8
294.4
308.3
328.2
136Nd
373.9
389.1
407.2
418.2
440.1
511.0
520.5
581.4
C.E.
602.4
669.1
705.9
206Pb
803
793.4
882.9
230.5*
198.5*
238.0*
266.8*
276.3*
306.4*
505.4*
540
553
580.5*
137Ba
72Ge
761.6*
781.5*
XBL736-3215

Fig. 2

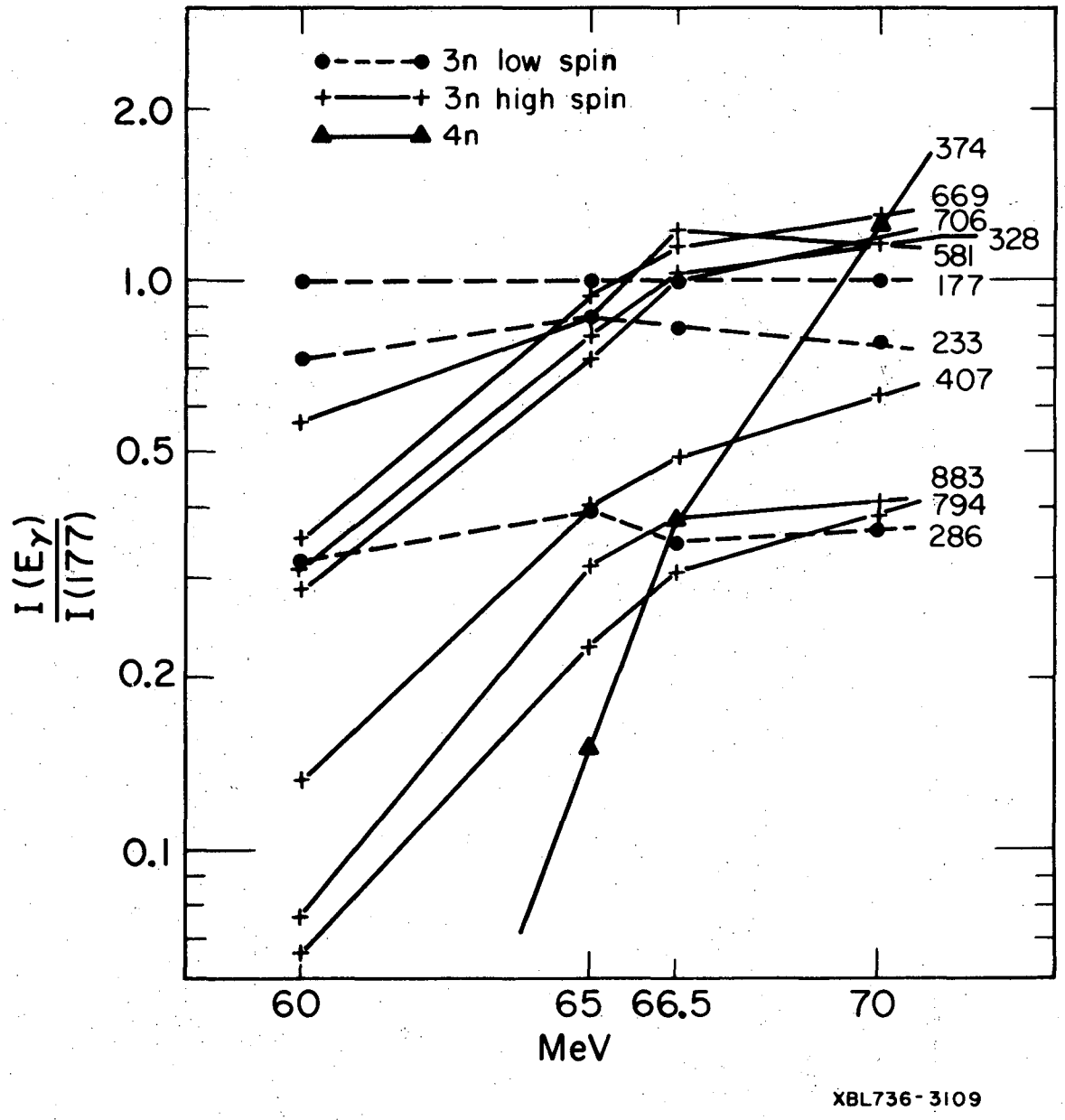
3n low spin
3n high spin
4n
2.0
1.0
0.5
0.2
0.1
I(Eγ)/I(177)
374
669
706
328
581
177
233
407
883
794
286
60
65
66.5
70
MeV
XBL736-3109

Fig. 3

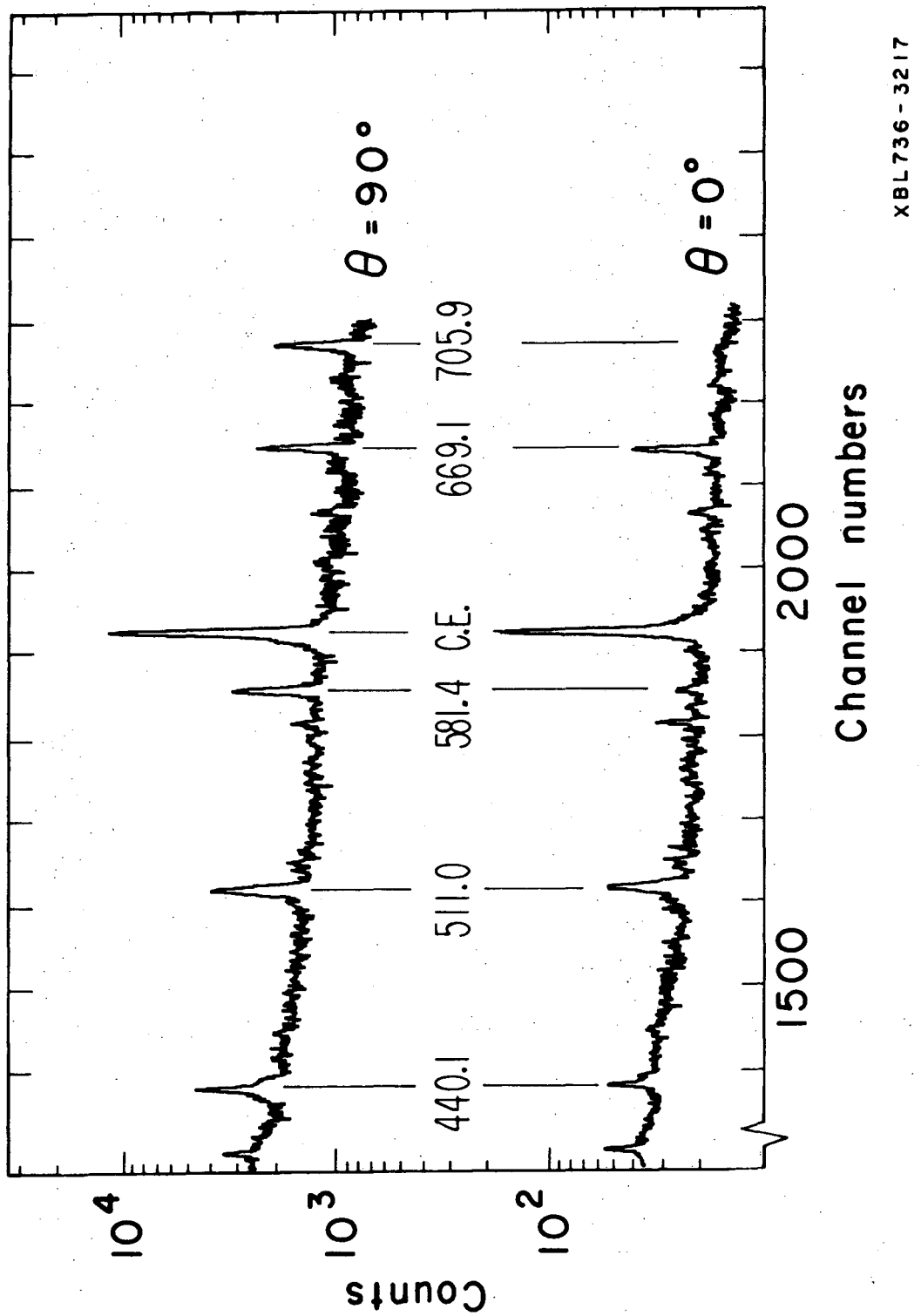
θ = 90°
θ = 0°
440.1
511.0
581.4 C.E.
669.1
705.9
1500
2000
Channel numbers
Counts
10^4
10^3
10^2
XBL736-3217

Fig. 4

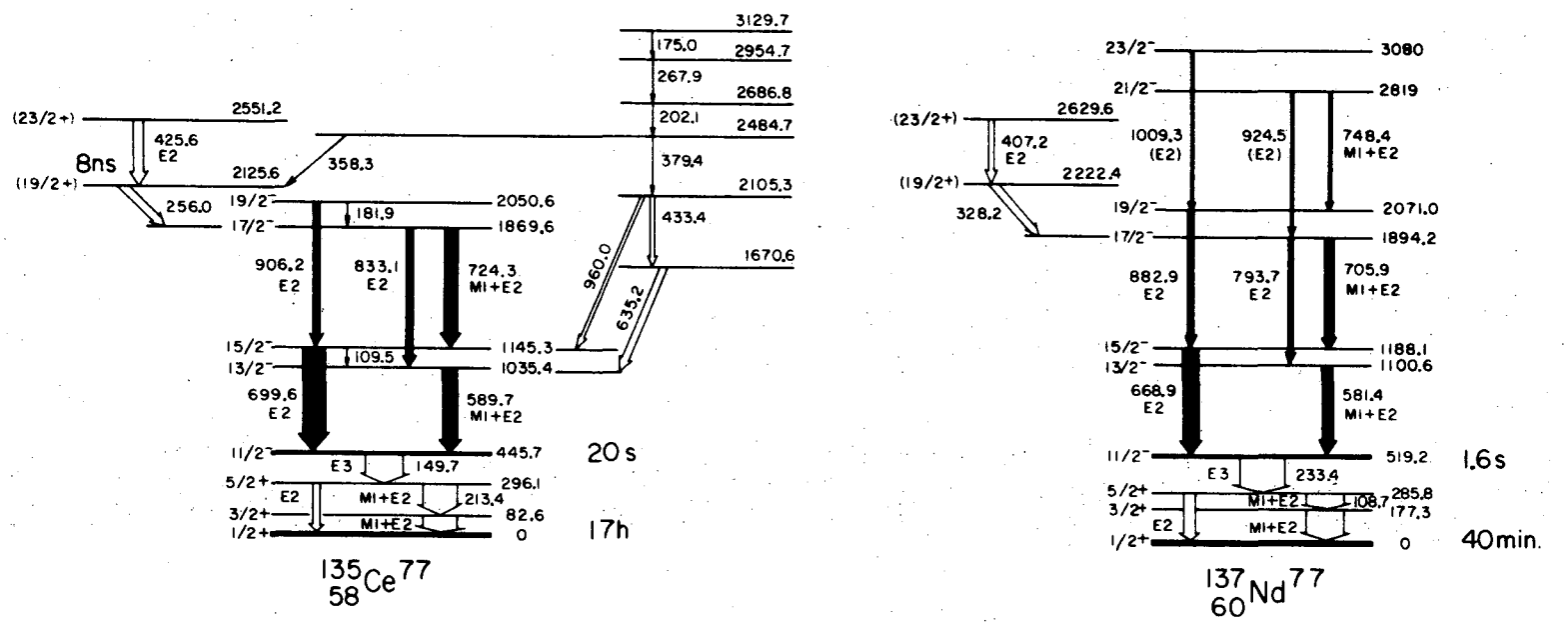
3129.7
175.0
2954.7
267.9
2686.8
202.1
2484.7
(23/2+)
2551.2
425.6
E2
8ns
(19/2+)
2125.6
358.3
379.4
2105.3
256.0
19/2⁻
2050.6
181.9
17/2⁻
1869.6
433.4
906.2
E2
833.1
E2
724.3
M1+E2
960.0
1670.6
635.2
15/2⁻
1145.3
109.5
13/2⁻
1035.4
699.6
E2
589.7
M1+E2
11/2⁻
445.7
20 s
E3
149.7
5/2+
296.1
E2
M1+E2
213.4
3/2+
82.6
M1+E2
1/2+
0
17h
135 58 Ce 77
23/2⁻
3080
21/2⁻
2819
(23/2+)
2629.6
1009.3
(E2)
924.5
(E2)
748.4
M1+E2
407.2
E2
(19/2+)
2222.4
328.2
19/2⁻
2071.0
17/2⁻
1894.2
882.9
E2
793.7
E2
705.9
M1+E2
15/2⁻
1188.1
13/2⁻
1100.6
668.9
E2
581.4
M1+E2
11/2⁻
519.2
1.6s
E3
233.4
5/2+
285.8
M1+E2
108.7
3/2+
177.3
E2
M1+E2
1/2+
0
40min.
137 60 Nd 77
XBL 736-3107

Fig. 5

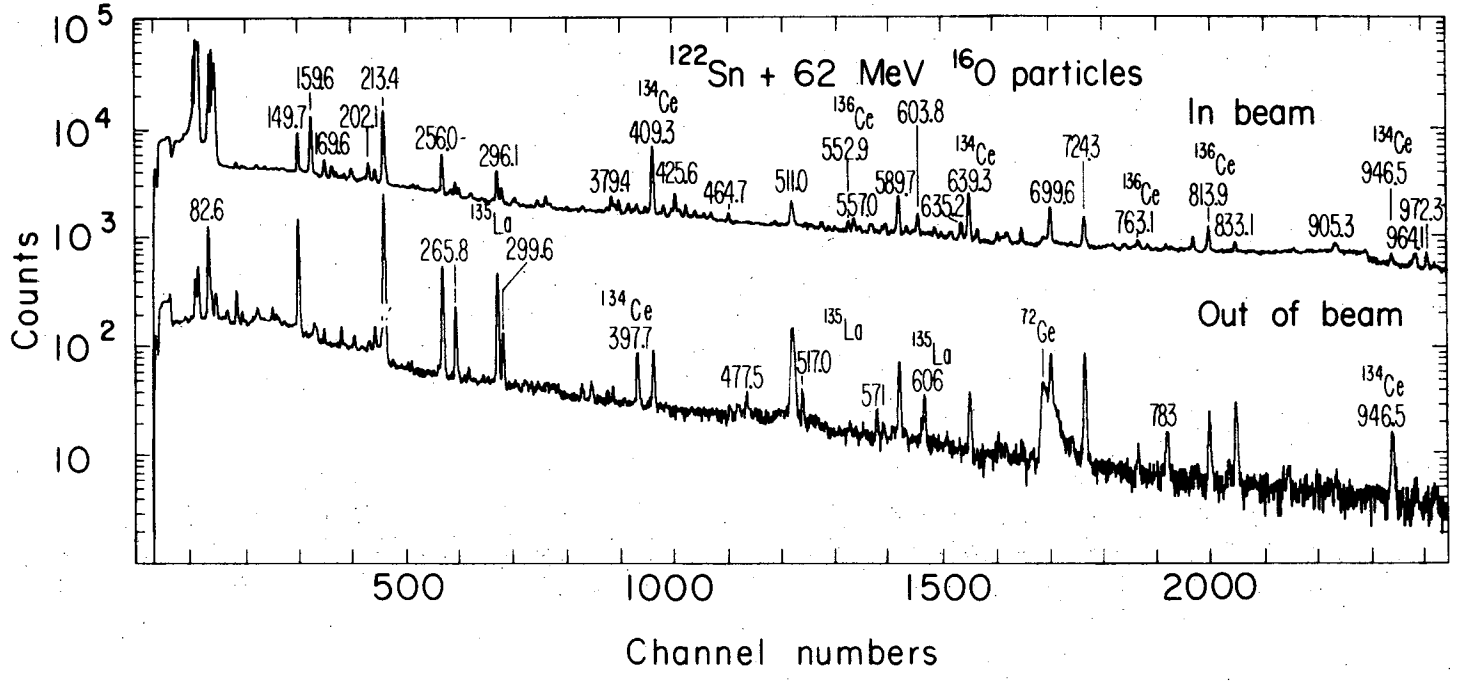

XBL736-3214

Fig. 6

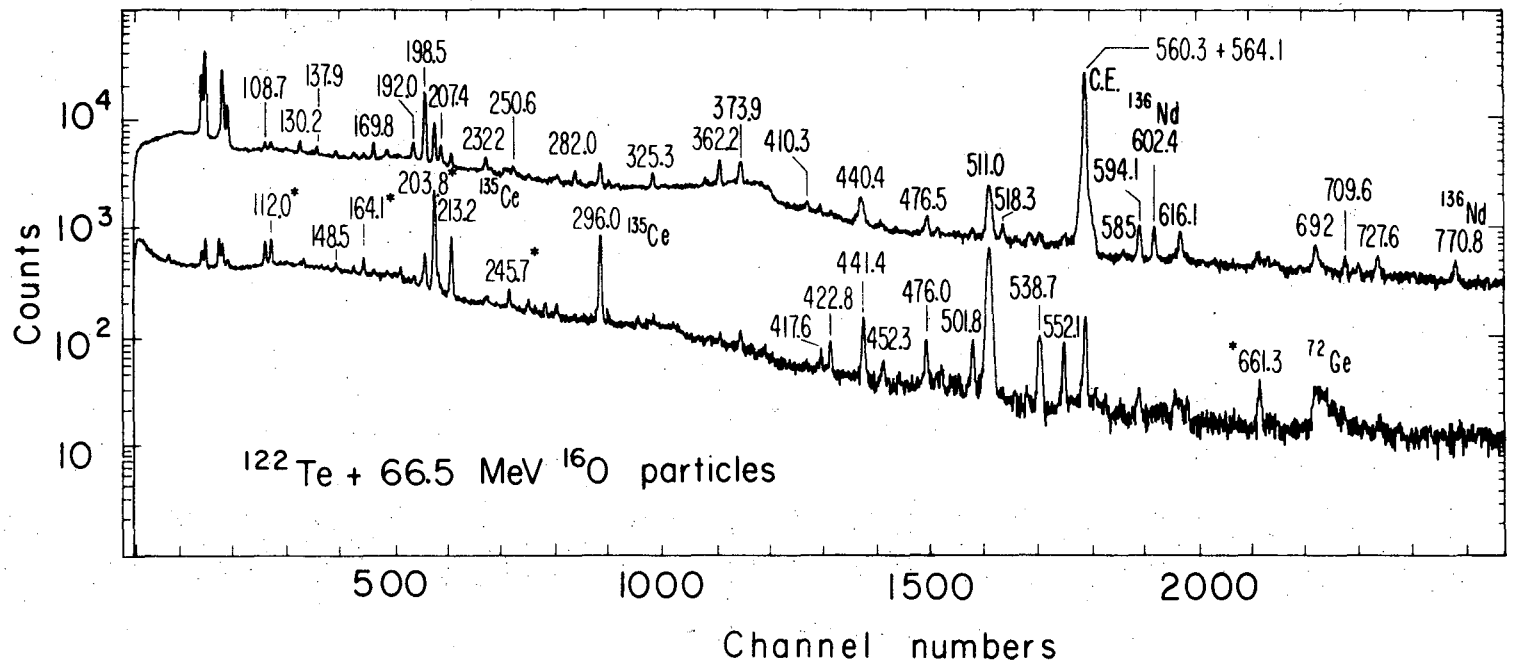

XBL736-3216

Fig. 7

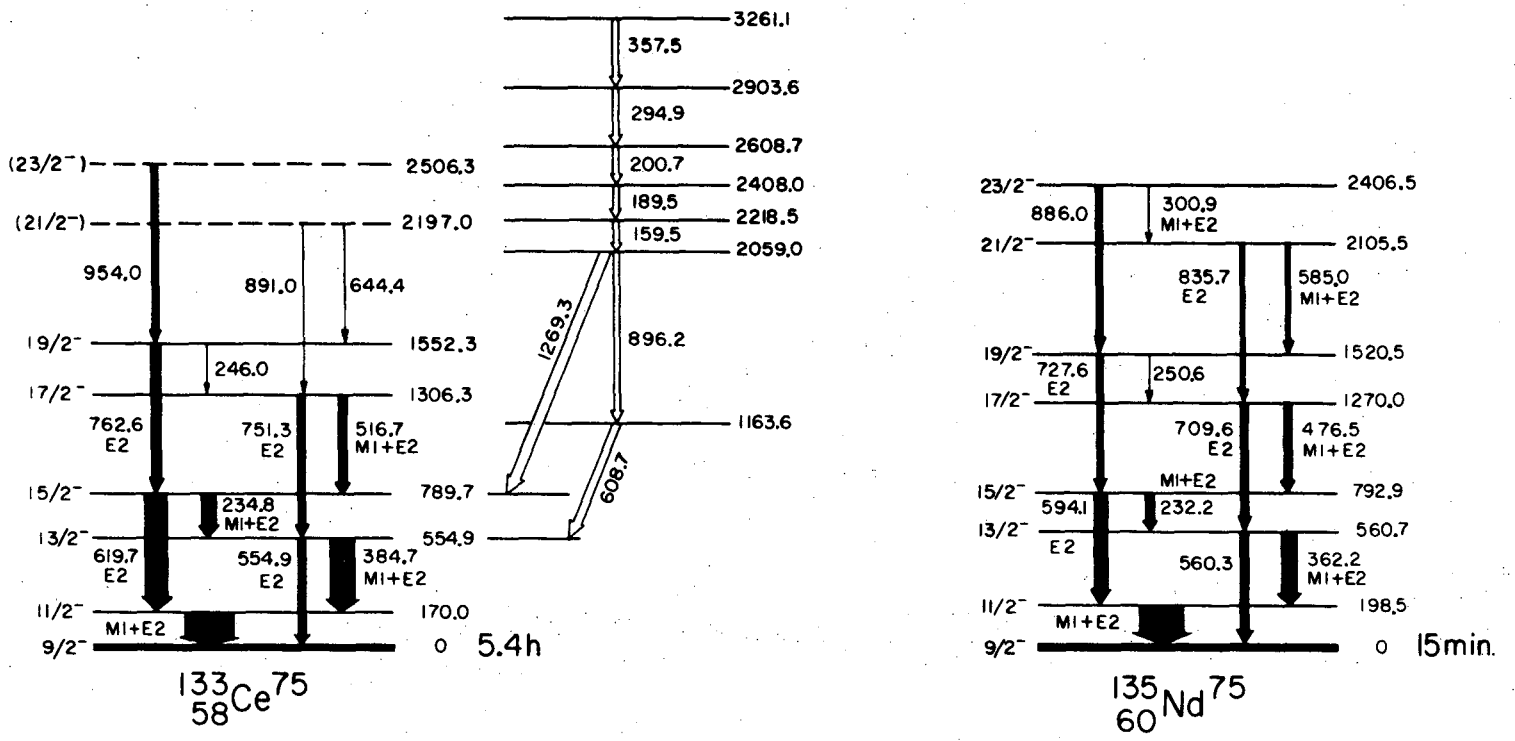
(23/2⁻) 2506.3
(21/2⁻) 2197.0
19/2⁻ 1552.3
17/2⁻ 1306.3
15/2⁻ 789.7
13/2⁻ 554.9
11/2⁻ 170.0
9/2⁻ 0 5.4h
954.0
891.0
644.4
246.0
762.6 E2
751.3 E2
516.7 M1+E2
234.8 M1+E2
619.7 E2
554.9 E2
384.7 M1+E2
M1+E2
$^{133}_{58}Ce^{75}$
3261.1
357.5
2903.6
294.9
2608.7
200.7
2408.0
189.5
2218.5
159.5
2059.0
1269.3
896.2
1163.6
608.7
23/2⁻ 2406.5
21/2⁻ 2105.5
19/2⁻ 1520.5
17/2⁻ 1270.0
15/2⁻ 792.9
13/2⁻ 560.7
11/2⁻ 198.5
9/2⁻ 0 15min.
886.0
300.9 M1+E2
835.7 E2
585.0 M1+E2
727.6 E2
250.6
709.6 E2
476.5 M1+E2
M1+E2
594.1 E2
232.2
560.3
362.2 M1+E2
M1+E2
$^{135}_{60}Nd^{75}$
XBL736-3108

Fig. 8

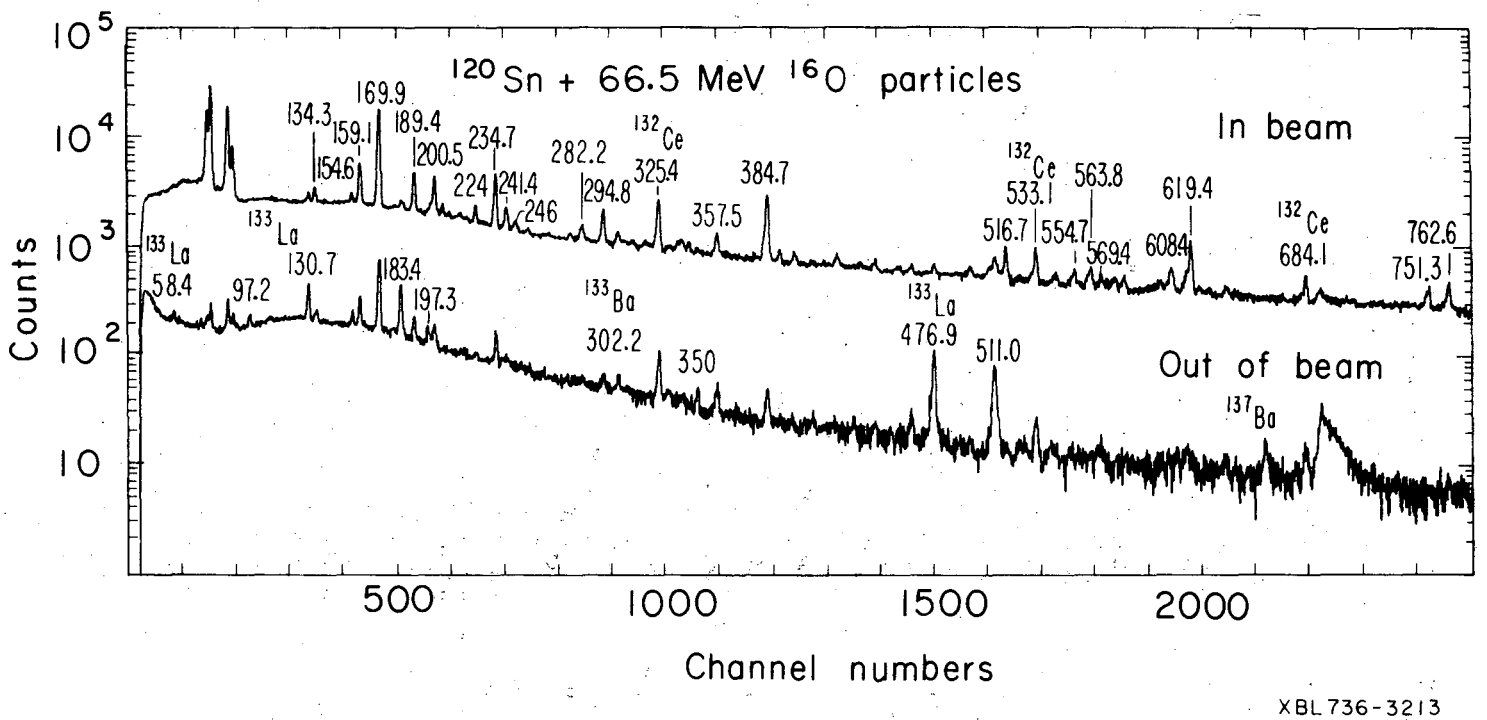

XBL 736-3213

Fig. 9

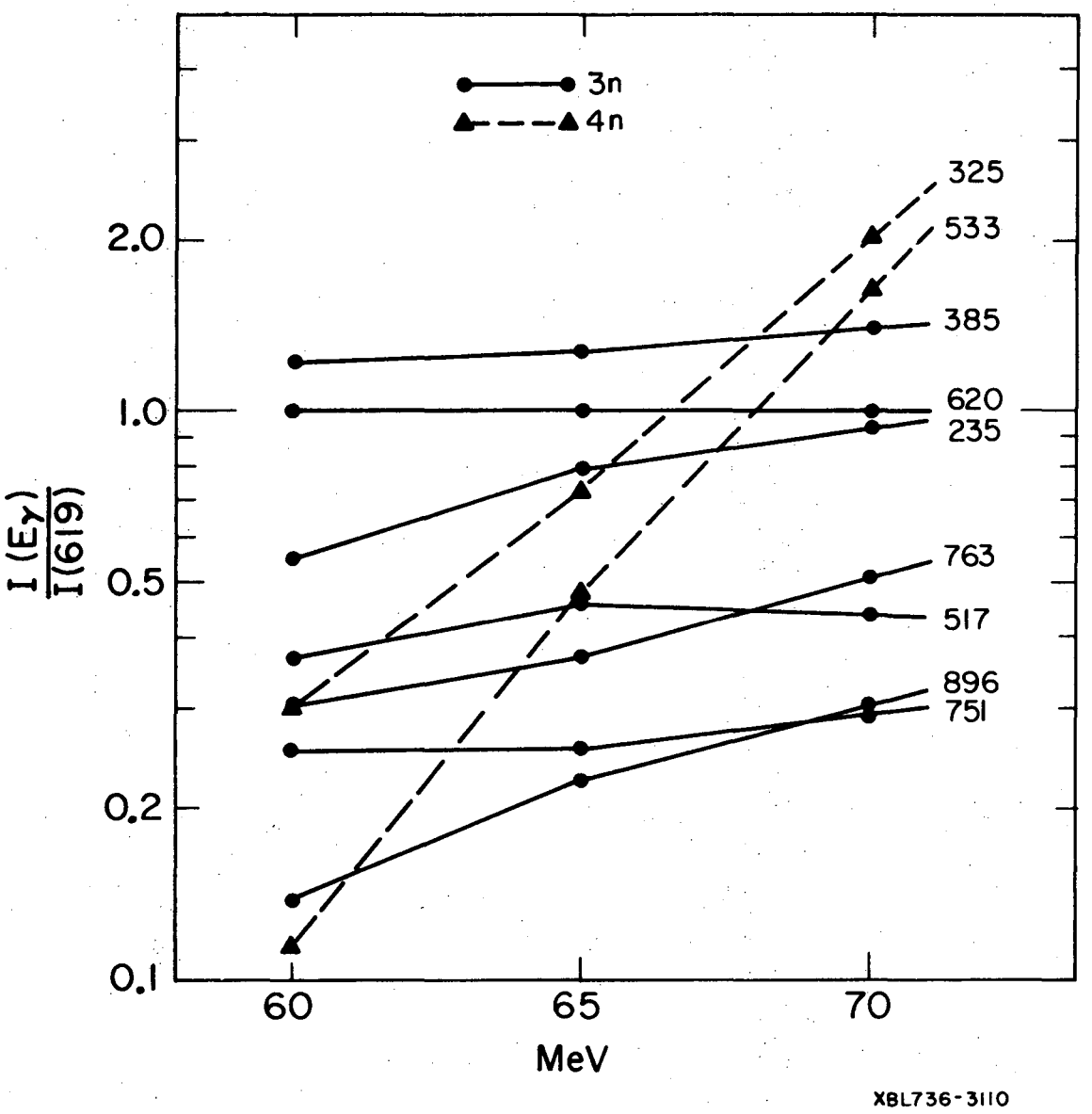
3n
4n
325
533
385
620
235
763
517
896
751
2.0
1.0
0.5
0.2
0.1
I (Eγ) / I(619)
60
65
70
MeV
XBL736-3110

Fig. 10

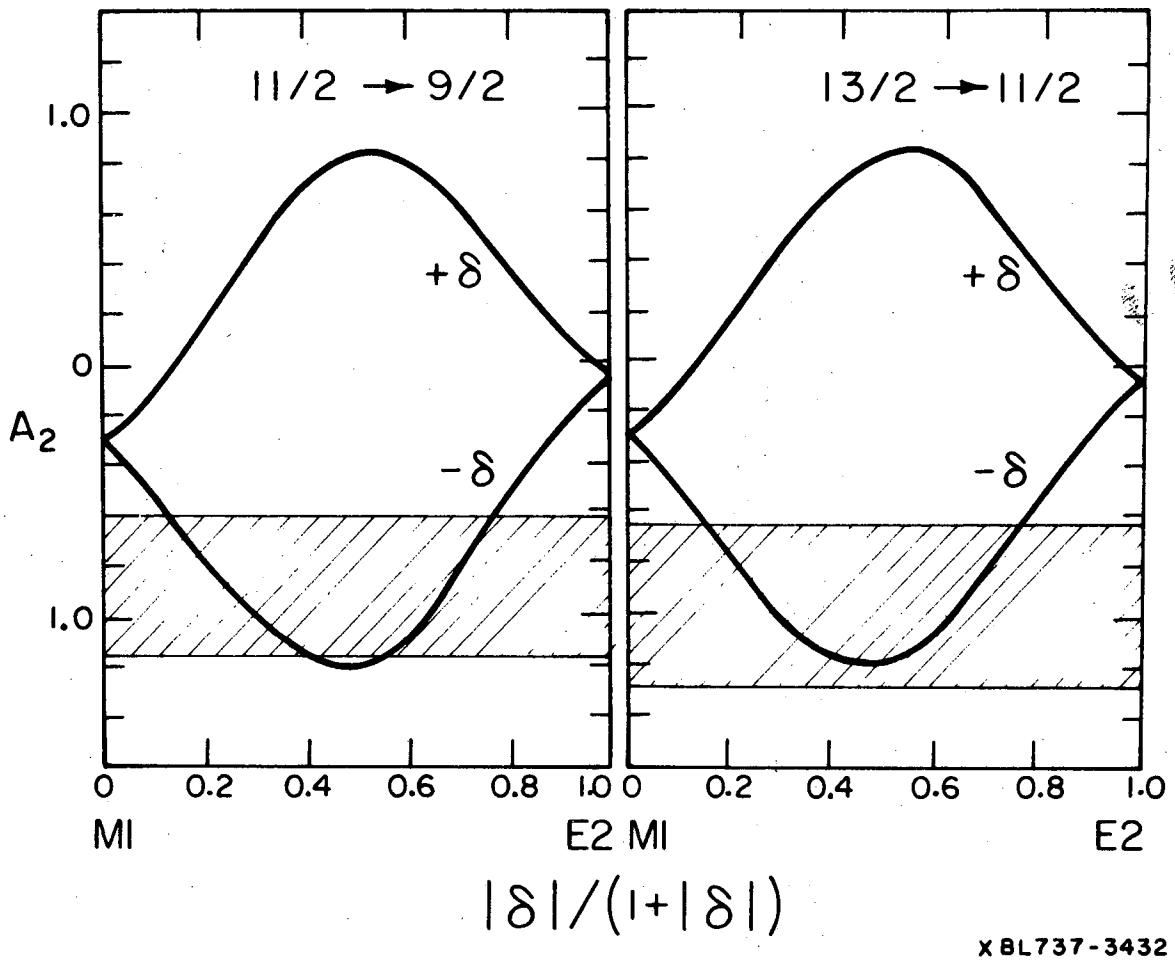
11/2 → 9/2
13/2 → 11/2
1.0
0
1.0
A_2
+δ
-δ
+δ
-δ
0
0.2
0.4
0.6
0.8
1.0
0
0.2
0.4
0.6
0.8
1.0
MI
E2
MI
E2
|δ|/(1+|δ|)
XBL737-3432

Fig. 11

LEGAL NOTICE

This report was prepared as an account of work sponsored by the United States Government. Neither the United States nor the United States Atomic Energy Commission, nor any of their employees, nor any of their contractors, subcontractors, or their employees, makes any warranty, express or implied, or assumes any legal liability or responsibility for the accuracy, completeness or usefulness of any information, apparatus, product or process disclosed, or represents that its use would not infringe privately owned rights.

TECHNICAL INFORMATION DIVISION
LAWRENCE BERKELEY LABORATORY
UNIVERSITY OF CALIFORNIA
BERKELEY, CALIFORNIA 94720